# Power factor correction AC-DC boost converter using PI-hysteresis current control

**Mariam K. Shehata[1], Hossam E. Mostafa Attia[1], Basem E. Elnaghi[2], Nagwa F. Ibrahim[1]**
[1]Department of Power and Electrical Machines, Faculty of Technology and Education, Suez University, Suez, Egypt
[2]Department of Electrical Engineering, Faculty of Engineering, Suez Canal University, Ismailia, Egypt

| Article Info | ABSTRACT |
|---|---|
| | The AC line input voltage is frequently rectified by single-phase diode rectifiers and filtered using sizable electrolytic capacitors. The capacitor draws current in brief pulses, so harmonics distort the line current, resulting in high losses. Harmonics and line current distortions harm the unity power factor and efficiency. This article adopts a simple single-stage AC-DC converter with a high-power factor and low total harmonic distortion. The PI hysteresis current control was utilized to reduce the total harmonic distortion and increase the power factor at full load. The PI controller was added to the outer voltage loop to regulate the output voltage. Ziegler-Nichol's tuning method was used to determine the controller gain levels. Simulation results were obtained for the AC-DC converter at a constant switching frequency to show the benefits of the proposed control method, which has a low total harmonic distortion and a high-power factor compared with cases without a controller. The proposed control method is accurate and efficient for achieving the power factor correction converter. Besides, the proposed control was stable during dynamic and steady-state responses. |
| | |

*Corresponding Author:*

Mariam K. Shehata
Department of Power and Electrical Machines, Faculty of Technology and Education, Suez University
Suez, El-Salam 43512, Egypt
Email: mariam.shehata@ind.suezuni.edu.eg

## 1. INTRODUCTION

Single-phase diode rectifiers are used in industrial applications, where the AC line input voltage is rectified and filtered using large electrolytic capacitors. This process, which includes nonlinear and storage components, generates harmonics and line current distortions. Total harmonic distortion (THD) is the term for these defects that harm the unity power factor (UPF) and efficiency. Power factor correction (PFC) and efficiency have taken on greater significance for power converters, and PFC converters are typically used to address line current harmonic issues with rectifiers [1]. Power factor (PF) is the cosine of the phase angle between the current and voltage waveforms for pure sine waves. It is required for AC-DC converters to meet international standards like IEC 61000-3-2 and IEEE-519. PFC can lower harmonics in the line current, improve power system capacity and efficiency, and lower user utility expenditures. Desirable PFC technique characteristics can be split into two categories: features on the input side include sinusoidal input current with nearly one-to-one PF functioning, reduced EMI filters, and insensitivity to minor signal disturbances in the load. In contrast, the output characteristics include good line and load control, minimal output voltage ripple, quick output dynamics (i.e., high bandwidth), and numerous output voltage levels if required by the application [2], [3]. Passive and active PFC are the two major approaches to power factor correction.

Passive PFC uses the inductive filter method, which requires an inductor to be placed between the rectifier output and the capacitor. Choosing the inductance value depends on the operation mode. The

resonance input filter method uses a series filter, which can achieve a high PF of 0.94. Passive PFC has drawbacks, including a large reactive element size, high THD, a lower PF compared to active schemes, and a lack of cost-effectiveness [2].

Active PFC techniques can be classified into buck, boost, buck-boost, SEPIC, and cuk converter [4]–[10]. These converters provide simple configurations for various input and output voltage conversion ratios. In contrast, control methods can be classified according to the input current control method, such as average current, peak current, and hysteresis current control (HCC) [11]–[13]. Some techniques can be used to perform the voltage or current control, such as sliding, predictive, passivity, and fuzzy logic control [14]–[18]. Active PFC techniques have the following advantages: lower harmonic content in the input current compared to the passive methods, a reduced root mean square (RMS) current rating of the output filter capacitor, and a UPF equal to 0.99 with a THD of 3% to 5%. Finally, active PFC techniques will outperform passive PFC techniques in size, weight, and cost for higher power levels. Many topologies are used to achieve PFC, as shown in Figure 1. The non-isolated type is also used in low and medium-power applications. There are differences in the operating modes and control methods used for each converter, including modes such as continuous conduction mode (CCM), discontinuous conduction mode (DCM), and boundary conduction mode (BCM). The DC-DC circuit converter changes a DC voltage difference to a higher or lower level. The voltage regulator is commonly used in switch-mode power supply (SMPS) applications. In this paper, section 2 introduces the boost topology design and operation. Section 3 presents the proposed system using PI-HCC of the boost PFC converter. Section 4 presents the simulation results and discussions for the proposed method. Finally, the conclusions for this paper are given in section 5.



Figure 1. Power converter topologies: (a) non isolated power topology and (b) isolated power topology

## 2. DESIGN AND OPERATION OF THE BOOST CONVERTER

While the switch is on, as shown in Figure 2, it represents a short circuit and should provide zero resistance to the current flow. As a result, the entire current will flow through the switch and back to the AC input source when the switch is on. It is assumed that the switch is turned on for a time $T_{on}$ and turned off for a time $T_{off}$. The inductor's polarity is switched around in this mode, as shown in Figure 3. The polarity switching keeps the current flowing in the same direction through the load and steps up the output voltage because the inductor, in this case, serves as a source in addition to the input source. The energy stored in the inductor is released and dissipated in the load resistance [19]. The boost converter's transfer function, the duty cycle ($D$), and the LC filter are determined as follows [20]:

$$\frac{V_o}{V_{in}} = \frac{T_s}{T_{off}} = \frac{1}{1-D} \tag{1}$$

where $V_{in}$ is the input voltage, $V_o$ is the desired output voltage, and $T_s$ is the time switching. $D$ is determined by (2):

$$D = 1 - \frac{V_{in}*\eta}{V_o} \tag{2}$$

$\eta$ is the boost converter's efficiency, estimated to be 80%. The inductor's value can be calculated by (3),

$$L = \frac{V_{in}*(V_o-V_{in})}{\Delta I_l*F_s*V_o} \tag{3}$$

where $\Delta I_l$ is the inductor's ripple current, and $F_s$ is the lowest switching frequency. Since the inductor is unknown, it is impossible to determine the ripple current, hence, 20% to 40% of the output current ($I_o$) is a fair range to use as a good approximation for the inductor ripple current in (4),

$$\Delta I_l = (0.2 \text{ to } 0.4) * I_{o(max)} * \frac{V_o}{V_{in}} \tag{4}$$

where $I_{o(max)}$ is the maximum output current necessary in the application, and the output's capacitor $C_{o(min)}$, which is selected according in (5):

$$C_{o(min)} = \frac{I_{o(max)}*D}{F_s*\Delta V_o}$$

(5)

where $\Delta V_o$ is the desired output voltage ripple, the equivalent series resistance of the used output's capacitor (*ESR*) causes more ripples in the output voltage, as given in (6):

$$\Delta V_{o(ESR)} = ESR(\frac{I_{o(max)}}{1-D} + \frac{\Delta I_l}{2})$$

(6)

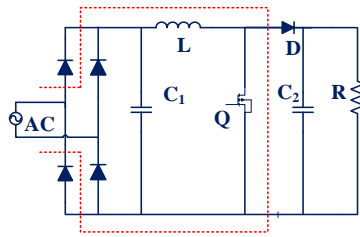where $\Delta V_{o(ESR)}$ is the additional output voltage ripple due to the capacitor's *ESR*.
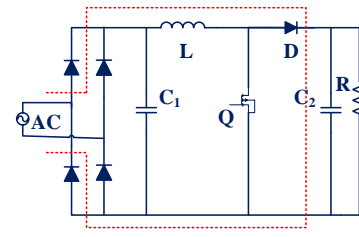


Figure 2. ON-switch boost converter



Figure 3. OFF- switch boost converter

## 3.    RESEARCH METHOD

This work aims to measure PF and THD values in the case of a resistive load, which was used with the boost converter. The applied input was a single-phase source with a frequency of 50 Hz. The AC input side was connected to a full-wave rectifier to convert the voltage from the AC form to the DC form for the designed voltage value. The prime purpose of the boost converter type is to raise the value of $V_o$ to a higher value, which is determined based on $D$. The boost converter topology has remarkable advantages, such as its simple design and continuous current form at either the input or output sides.

The PI control was adopted in this work to reduce THD and improve PF. $K_p$ and $K_i$ gains of the controller were adjusted using Ziegler Nichol's tuning method to achieve PFC. Figure 4 illustrates the proposed PI hysteresis current control Simulink model. In contrast, the output is connected to a PI controller to obtain an accurate value for $V_o$, low THD, and a high PF. The inductor current $I_l$ can be obtained depending on the sensed $V_{in}$ and $V_o$, as shown in Figure 4. The boost converter has two distinct states: The $T_{on}$, in which the switch is closed, and the $T_{off}$, in which the switch is made open. The estimated $I_l(t)$ can be expressed as in (7) and (8).

$$L\frac{dI_l}{d_t} = V_{in}(t)$$

(7)

$$L\frac{dI_l}{d_t} = V_{in} - V_o$$

(8)

Since the $I_l(t)$ can be obtained by integrating the two states. The boost inductor current is continuously compared with the reference current waveform obtained from the voltage control loop, and the error signal after amplification is fed to the hysteresis comparator. When the actual inductor current goes above the reference current, the comparator changes its state to switch off the boost switch and the current ramp goes down. When the actual current falls below the reference current, it changes states again and turns the boost switch on. Figure 5 depicts the current control scheme's general hysteresis for 5(a) functional diagram and 5(b) current and PWM waveforms. The basic equations of reference current ($I_{ref}$) and controller output ($U$) for the PI-HCC method are given in (9) and (10) [1],

$$I_{ref} = \frac{(V_{ref}-V_o)(K_p+\frac{K_i}{S})I_l}{V_{rms}^2}$$

(9)

$$U = (I_{ref} - I_l)(K_p + \frac{K_i}{S})$$

(10)

where $V_{ref}$ is the reference voltage, and $V_{rms}$ is the input voltage root mean square.
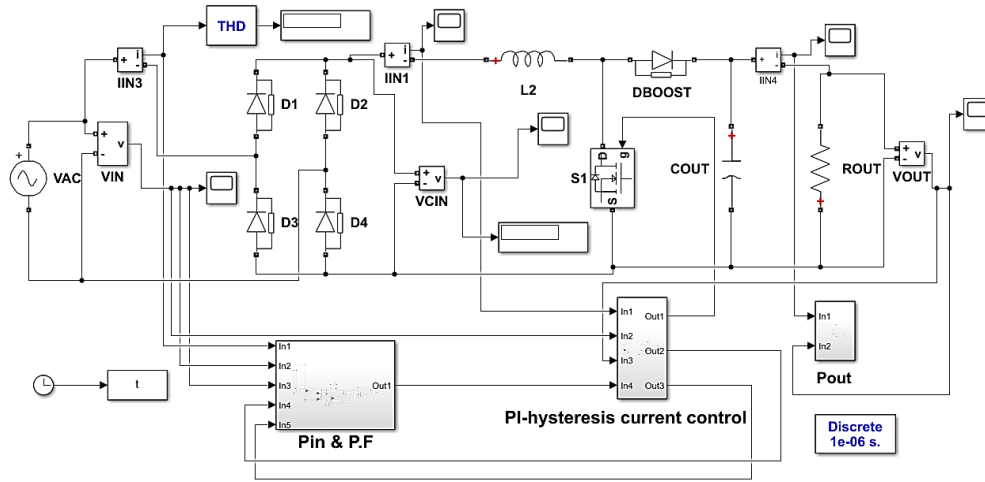
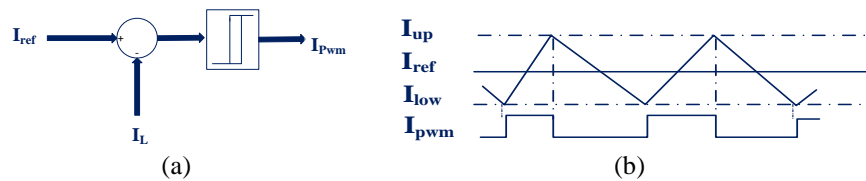Figure 4. PI-HCC Simulink model for PFC boost converter



Figure 5. HCC scheme (a) functional diagram and (b) current and PWM waveforms

## 4. SIMULATION RESULTS AND DISCUSSION

Simulation is done using MATLAB/Simulink for a single-phase AC-DC converter. The PI-controlled compensator drives the outer loop, and the current-controlled PI controller powers the inner current loop. The entire system is simulated while considering the specifications listed in Table 1. The average current control published in [21] was re-simulated to confirm the simulation methodology validity adopted in this study. It was noticed that both the re-simulation results and the published results were identical. The relevant curves of the re-simulation results are inserted in the supplementary materials.

Table 1. Specification and components used in the simulation of AC-DC boost converter

| Parameter | Symbol | Value | Unit |
|---|---|---|---|
| Input voltage | $V_{in}$ | 40 | V(RMS) |
| Supply frequency | $F$ | 50 | Hz |
| Output voltage | $V_o$ | 100 | V |
| Load | $R$ | 100 | Ω |
| Capacitor | $C_o$ | 1000 | μF |
| Inductor | $L$ | 3 | mH |
| Output power | $P_o$ | 100 | W |
| Switching frequency | $F_s$ | 21 | kHz |

Before applying the proposed control technique, the traditional system showed that PF was 0.9245, 0.9245, and 0.9983 for the R, RL, and RLC loads, respectively. Furthermore, the THD level was 63.85%, 63.87%, and 71.92% for the same loads. After applying the proposed control technique, R of 100 Ω was used as a 100% load for the simulation, as shown in Table 2. Figures 6(a)-(f) shows the simulated results since (a) $I_{in}$ & $V_{in}$, (b) $I_o$ & $V_o$, (c) $I_R$ & $V_R$, (d) $P_{in}$ & $P_o$, (e) *THD* %, and (f) *PF*. The simulation results show that the proposed system for the PFC boost converter with PI control for the resistive load is efficient. The PI control technique was used to regulate the output voltage at 100 V and achieve a sinusoidal form for the input current in the AC-DC boost converter. Hence, the PI control offers a limited THD, and the PF is close to the correct one. As a result, the system would be applicable in various industrial applications, whether the load is linear or non-linear. The simulation results of the PI control with the R load are listed in Table 2. Moreover, Table 3 compares the re-simulated results with the proposed system in this study.
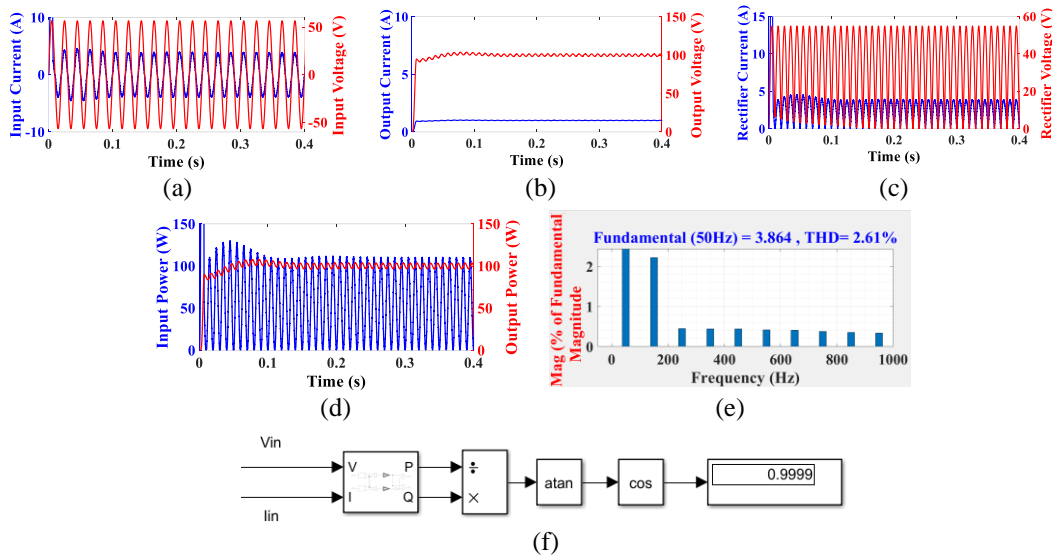
Figure 6. Steady-state response for PFC boost converter (a) $I_{in}$ & $V_{in}$, (b) $I_o$ & $V_o$, (c) $I_R$ & $V_R$, (d) $P_{in}$ & $P_o$, (e) THD %, and (f) *PF*

Table 2. Simulation results for the boost converter PI-HCC with R load

| Parameter | Symbol | Value | Unit | Parameter | Symbol | Value | Unit |
|---|---|---|---|---|---|---|---|
| Peak input voltage | $V_{in}$ | 56.56 | V | Input power | $P_{in}$ | 110 | W |
| Supply frequency | $F$ | 50 | Hz | Output power | $P_o$ | 100 | W |
| Output voltage | $V_o$ | 100 | V | Rectifier current | $I_R$ | 3.9 | A |
| Load | $R$ | 100 | Ω | Rectifier voltage | $V_R$ | 54.92 | V |
| Input current | $I_{in}$ | 4 | A | Power factor | PF | 0.9999 | - |
| Output current | $I_o$ | 1 | A | Total harmonic distortion | THD | 2.61 | % |

This study aims to achieve a high PF and a low THD, which increases the efficiency of the boost converter for different applications, such as switching mode power supplies and LED gate drive circuits. This goal was efficiently achieved using an uncomplicated proposed design. In contrast, some complex designs and control methods were presented in [6], which recently introduced a literature review for the boost converter topology, such as the traditional bridge boost converter with PFC, PFC with pseudo-continuous conduction, interleaved PFC, hybrid interleaved PFC, and PFC with a bidirectional switch. However, detailed the emerging disadvantages of such topologies, which include difficulty in implementing control, high cost, and the complexity of the design with high distortions for the used topologies with the boost converter, affecting the efficiency and performance of the converter in various power applications [6], [22]–[24]. Moreover, the proposed design was modified to improve the performance since PF and THD showed 0.9999 and 2.61%, respectively, which is better than those who adopted the same topology as our work in [21], [25]. The adopted average current control method in [21] has some demerits, such as the following: the inductor's current must be sensed, which is a difficult task, and the current mode control system requires the use of the current error amplifier. Besides, a compensation network must be constructed that considers the variable operating points of the converter that uses the error amplifier. Published results of [21] indicated 3.49% and 0.99972 of the THD and the PF, respectively.

Table 3. Comparison results between re-simulated results and the proposed for boost converter R load

| Refs | Control Technique | Topology | Input voltage (V) | Output Voltage (V) | Supply frequency (Hz) | Load (Ω) | Input current (A) | Output current (A) | THD (%) | P. F |
|---|---|---|---|---|---|---|---|---|---|---|
| [21] | PI average current control | Boost | 56.56[*] | 100[*] | 50[*] | 100[*] | 4.2[*] | 1.02[*] | 6.81[*] | 0.9997[*] |
| This work | PI hysteresis current control | Boost | 56.56 | 100 | 50 | 100 | 4 | 1 | 2.61 | 0.9999 |

[*]Re-simulated result

In contrast, the adopted HCC has the following advantages: a compensating ramp is unnecessary, and the input current waveforms have little distortion. A comparison is introduced here between the most

important results obtained from this work and the published results in the literature. This comparison is presented in Table 4 for the R load. The current work aims to achieve a high PFC with the lowest harmonic ratio through a simple and easy control technique with high efficiency. This objective was achieved using the Simulink platform of MATLAB.

Table 4. Comparison results between refs [21], [25], and the proposed for boost converter R load

| Refs | Control Technique | Topology | THD (%) | P. F | $V_o$ (V) |
|---|---|---|---|---|---|
| [21] | PI average current control | Boost | *6.81 | 0.9997 | 100 |
|  |  |  | +3.49 | 0.99 | 100 |
| [25] | Peak current control | Boost | 3.08 | 0.99 | 400 |
|  | Hysteresis current control | Boost | 4.28 | 0.99 | 400 |
| This work | PI hysteresis current control | Boost | 2.61 | 0.9999 | 100 |

*Re-simulated result, +Published result

## 5.    CONCLUSION

This paper has proposed a single-stage AC–DC converter with a high PF and low THD. Besides, the proposed converter's analysis, design, and simulation results have also been presented. The proposed converter is a PFC boost converter with PI-HCC. The proposed converter has a simple design and a reasonable price for practical use. As a result of this, the suggested converter is appropriate for various power applications. By utilizing the proposed control for the PFC boost converter, the proposed converter has a high PF of 0.9999 and low THD to comply with IEC 61000-3-2 harmonic regulation. The PFC buck and buck-boost type AC-DC converters can be operated in CCM using the PI-HCC. The proposed converter offers a low THD of 2.61% at full load thanks to the single-stage converter. In the future, it is planned to investigate this system experimentally since the proposed system was successfully achieved in the research thanks to the Simulink platform of MATLAB.

## REFERENCES

[1]   Z. Ortatepe and A. Karaarslan, "DSP-based comparison of PFC control techniques applied on bridgeless converter," *IET Power Electronics*, vol. 13, no. 2, pp. 317–323, Feb. 2020, doi: 10.1049/iet-pel.2018.5411.
[2]   Y. Wei, Q. Luo, J. M. Alonso, and A. Mantooth, "A magnetically controlled single-stage AC–DC converter," *IEEE Transactions on Power Electronics*, vol. 35, no. 9, pp. 8872–8877, Sep. 2020, doi: 10.1109/TPEL.2020.2970589.
[3]   G. G. Ramanathan and N. Urasaki, "Non-isolated interleaved hybrid boost converter for renewable energy applications," *Energies*, vol. 15, no. 2, p. 610, Jan. 2022, doi: 10.3390/en15020610.
[4]   X. Liu, Y. Wan, M. He, Q. Zhou, and X. Meng, "Buck-type single-switch integrated PFC converter with low total harmonic distortion," *IEEE Transactions on Industrial Electronics*, vol. 68, no. 8, pp. 6859–6870, 2021, doi: 10.1109/TIE.2020.3007121.
[5]   H. Luo, J. Xu, D. He, and J. Sha, "Pulse train control strategy for CCM boost PFC converter with improved dynamic response and unity power factor," *IEEE Transactions on Industrial Electronics*, vol. 67, no. 12, pp. 10377–10387, Dec. 2020, doi: 10.1109/TIE.2019.2962467.
[6]   J. R. Ortiz-Castrillón, G. E. Mejía-Ruíz, N. Muñoz-Galeano, J. M. López-Lezama, and S. D. Saldarriaga-Zuluaga, "PFC single-phase AC/DC boost converters: bridge, semi-bridgeless, and bridgeless topologies," *Applied Sciences*, vol. 11, no. 16, p. 7651, Aug. 2021, doi: 10.3390/app11167651.
[7]   T. Bang and J.-W. Park, "Development of a ZVT-PWM buck cascaded buck–boost PFC converter of 2 kW with the widest range of input voltage," *IEEE Transactions on Industrial Electronics*, vol. 65, no. 3, pp. 2090–2099, Mar. 2018, doi: 10.1109/TIE.2017.2739703.
[8]   C. R. Fotso Mbobda and A. M. Dikandé, "A dual-switch cubic SEPIC converter with extra high voltage gain," *International Journal of Power Electronics and Drive Systems (IJPEDS)*, vol. 12, no. 1, p. 199, 2021, doi: 10.11591/ijpeds.v12.i1.pp199-211.
[9]   X. Lin, Z. Jin, F. Wang, and J. Luo, "A novel bridgeless cuk PFC converter with further reduced conduction losses and simple circuit structure," *IEEE Transactions on Industrial Electronics*, vol. 68, no. 11, pp. 10699–10708, Nov. 2021, doi: 10.1109/TIE.2020.3031527.
[10]  M. A. Z. A. Rashid, A. Ponniran, M. K. R. Noor, J. N. Jumadril, M. H. Yatim, and A. N. Kasiran, "Optimization of PFC cuk converter parameters design for minimization of THD and voltage ripple," *International Journal of Power Electronics and Drive Systems (IJPEDS)*, vol. 10, no. 1, p. 514, Mar. 2019, doi: 10.11591/ijpeds.v10.i1.pp514-521.
[11]  K. Naraharisetti, J. Channegowda, and P. B. Green, "Design and modeling of CCM average current control PFC AC-DC boost converter," in *2021 IEEE Green Technologies Conference (GreenTech)*, Apr. 2021, pp. 403–408, doi: 10.1109/GreenTech48523.2021.00069.
[12]  Y. Liu, H. Zhang, H. Wang, H. Dan, M. Su, and X. Pan, "Peak and valley current control for cuk PFC converter to reduce capacitance," *IEEE Transactions on Power Electronics*, vol. 37, no. 1, pp. 313–321, Jan. 2022, doi: 10.1109/TPEL.2021.3099218.
[13]  J.-J. Chen, Y.-S. Hwang, Y. Ku, Y.-H. Li, and J.-A. Chen, "A current-mode-hysteretic buck converter with constant-frequency-controlled and new active-current-sensing techniques," *IEEE Transactions on Power Electronics*, vol. 36, no. 3, pp. 3126–3134, Mar. 2021, doi: 10.1109/TPEL.2020.3017809.
[14]  M. A. F. Al-Qaisi, M. A. Shehab, A. Al-Gizi, and M. Al-Saadi, "High performance DC/DC buck converter using sliding mode controller," *International Journal of Power Electronics and Drive Systems*, vol. 10, no. 4, pp. 1806–1814, 2019, doi: 10.11591/ijpeds.v10.i4.pp1806-1814.
[15]  A. Al Zawaideh and I. M. Boiko, "Analysis of stability and performance of a cascaded PI sliding-mode control DC–DC boost converter via LPRS," *IEEE Transactions on Power Electronics*, vol. 37, no. 9, pp. 10455–10465, Sep. 2022, doi: 10.1109/TPEL.2022.3169000.
[16]  C. González-Castaño, C. Restrepo, F. Sanz, A. Chub, and R. Giral, "DC voltage sensorless predictive control of a high-efficiency PFC single-phase rectifier based on the versatile buck-boost converter," *Sensors*, vol. 21, no. 15, p. 5107, Jul. 2021, doi: 10.3390/s21155107.
[17]  M. A. Hassan, E. Li, X. Li, T. Li, C. Duan, and S. Chi, "Adaptive passivity-based control of DC–DC buck power converter with constant power load in DC microgrid systems," *IEEE Journal of Emerging and Selected Topics in Power Electronics*, vol. 7, no. 3, pp. 2029–2040, Sep. 2019, doi: 10.1109/JESTPE.2018.2874449.

[18] S. Ozdemir, N. Altin, and I. Sefa, "Fuzzy logic based MPPT controller for high conversion ratio quadratic boost converter," *International Journal of Hydrogen Energy*, vol. 42, no. 28, pp. 17748–17759, Jul. 2017, doi: 10.1016/j.ijhydene.2017.02.191.

[19] R. W. Erickson and D. Maksimović, "Steady-state equivalent circuit modeling, losses, and efficiency," in *Fundamentals of Power Electronics*, Boston, MA: Springer US, 2001, pp. 39–61.

[20] B. Hauke, "Basic calculation of a boost converter's power stage," *Texas Instruments, Application Report November*, no. November 2009, pp. 1–9, 2009, [Online]. Available: http://scholar.google.com/scholar?hl=en&btnG=Search&q=intitle:Basic+Calculation+of+a+Boost+Converter's+Power+Stage#0.

[21] P. D. B. G. Samarth, "PFC boost topology using average current control method," *International Journal of Innovative and Emerging Research in Engineering*, vol. 3, no. 5, pp. 39–44, 2016.

[22] M. M. Subbarao, C. S. Babu, and S. Satyanarayana, "Charge current controlled single phase integrated switched mode power factor correction converter," *Energy Procedia*, vol. 117, pp. 71–78, Jun. 2017, doi: 10.1016/j.egypro.2017.05.108.

[23] A. Jha, V. Bist, and B. Singh, "A PFC modified-Landsman converter based PWM-Dimmable RGB HB-LED driver for large area projection applications," in *2015 IEEE IAS Joint Industrial and Commercial Power Systems / Petroleum and Chemical Industry Conference (ICPSPCIC)*, Nov. 2015, pp. 66–75, doi: 10.1109/CICPS.2015.7974055.

[24] G. A. Henao, J. A. Castro, C. L. Trujillo, and E. A. Narvaez, "Design and development of a LED driver prototype with a single-stage PFC and low current harmonic distortion," *IEEE Latin America Transactions*, vol. 15, no. 8, pp. 1368–1375, 2017, doi: 10.1109/TLA.2017.7994781.

[25] A. Karaarslan and I. Iskender, "The analysis of AC-DC boost PFC converter based on peak and hysteresis current control techniques," *International Journal on "Technical and Physical Problems of Engineering" (IJTPE)*, vol. 3, no. 2, pp. 100–105, 2011.

## BIOGRAPHIES OF AUTHORS

**Mariam K. Shehata** received the B.Sc. and M.Sc. degrees in Power and Electrical Machines technology from the Faculty of Technology and Education, Suez University, Egypt, in 2011 and 2018, respectively. She is currently pursuing a Ph.D. degree with the same faculty in the Power Electronics area. She was a Teaching Assistant with Suez University, from 2013 to 2019, where she is an Assistant Lecturer since 2019. Her current research interests include Power Converters and Control Techniques. She can be contacted at email: mariam.shehata@ind.suezuni.edu.eg.

**Hossam Eldin Mostafa Attia** received the B. Sc, M. Sc and Ph. D. from faculty of engineering, Ain Shams University, Cairo, Egypt in 1987, 1994 and 1999, respectively. From 1991 to 1997 worked in Egypt Air Company as second engineer. From 1997 to 2001, worked as a teacher assistant at College of Technological Studies - The Public Authority of Applied Education and Training-Kuwait Since 2001, I have been a faculty member with the Electrical Department at the Faculty of Industrial Education, Suez University, Suez, Egypt. Currently, working as a professor and Dean of faculty of Technology and Education since August 2019, Suez Univ. Egypt. He can be contacted at email: hossam.attia@ind.suezuni.edu.eg.

**Basem E. Elnaghi** received the B.Sc., M.Sc., and Ph.D. degrees in electrical power engineering in 2002 and 2009, and 2015 respectively, from Suez Canal University, Port Said, Egypt. Since 2015, he has been Associate professor with the electrical engineering Department, faculty of engineering, Suez Canal University. He joined the Department of faculty of engineering, Suez Canal University. His main interests include ac and dc drives, direct torque and field-oriented control techniques, and DSP control, control of electrical machines and wind energy conversion system, and power electronics applications. He can be contacted at email: Basem_elhady@eng.suez.edu.eg.

**Nagwa F. Ibrahim** received the B.S. from Faculty of Industrial Education. Suez Canal University, Suez, Egypt, in 2008, MSC. From Faculty of Industrial Education, Suez University, Suez, Egypt in 2015 and Ph.D. degree from faculty of industrial education, Suez University, Suez, Egypt in 2019. She is currently an assistant Professor with the Department of Electrical power and machine, Faculty of Technology and Education, Suez University. Her research interests are in the area of renewable energy sources, power system protection, power electronics, high voltage direct current (HVDC), control and power quality issues, control of power electronic converters and electrical machine drives. She can be contacted at email: Nagwa.ibrahim@ind.suezuni.edu.eg.